Talanta 86 (2011) 71–81

Contents lists available at ScienceDirect

Talanta

journal homepage: www.elsevier.com/locate/talanta

Uncertainty of ozone measurements with the primary standard reference photometer (SRP45)

Manuel A. Leiva G.[a,*], Consuelo Araya C.[a], Carlos Mancilla[b], Rodrigo Seguel[b], James E. Norris[c]

[a] Centro de Ciencias Ambiental, Facultad de Ciencias, Universidad de Chile, Casilla 653, Santiago, Chile
[b] Fundación CENMA, Avenida Larraín 9975, La Reina, Santiago, Chile
[c] Analytical Chemistry Division, National Institute of Standards and Technology, Gaithersburg, MD, USA

ARTICLE INFO

Article history:
Received 21 March 2011
Received in revised form 30 July 2011
Accepted 2 August 2011
Available online 1 September 2011

Keywords:
Primary standard reference photometer
SRP
Air quality
Uncertainty evaluation
GUM

ABSTRACT

A comparison of the ozone primary reference standard photometer serial number 45 (SRP45) against the National Institute of Standards and Technology (NIST) instruments, serial number 0 (SRP0) and 2 (SRP2), has been performed in order to establish the traceability and comparability of ozone measurements made by the Chilean atmospheric science community. A complete uncertainty budget was developed for SRP45, using a GUM approach. The results of the comparisons allow us to conclude that SRP45, SRP0 and SRP2 are comparable according to internationals criteria over an ozone mole fraction range of 0 nmol mol^{-1} to at least 500 nmol mol^{-1}. The official result for the validation of SRP45 is $x_{ozone}^{SRP45} = [0.013 + 0.99806 x_{ozone}^{SRP2}]$ nmol mol^{-1} with an expanded uncertainty of $2 \times \sqrt{(0.27)^2 + (1.18 \times 10^{-2} \times x_{ozone})^2}$ from 0 to 500 nmol mol^{-1}.

1. Introduction

Ozone is a secondary photochemical oxidant formed naturally by biogenic sources and is a common urban and regional air pollution problem in many parts of the world. A typical background ozone concentration can vary from 25 to 45 nmol mol^{-1} [1]. However, anthropogenic emissions may increase ozone levels in or near metropolitan areas [2–4]; it is well known that the resultant ozone can be harmful to human health [5,6] and plant-life [7] as well as cause damage to materials [8]. The monitoring of ambient ozone is an essential first step in understanding the processes and mechanisms of the formation of ozone [1,4].

The measurement equipment used for monitoring ambient ozone involves numerous analytical methods using entirely different principles [9]. The methods include electrochemical, colorimetric, chemiluminescence, photometric, spectroscopy, photoacoustic and Fourier transform infrared (FTIR) spectroscopy [10]. The photometric method is used extensively in field measurements because of its relative simplicity and low cost [11,12]. The UV photometry and chemiluminescent methods are currently the most accepted techniques for measuring atmospheric ozone and have been applied successfully to measure low concentrations of ozone at urban and non-urban sampling locations at surface level because of its relative effortlessness and the possibility of using it for the development of a primary reference standard [13–15].

The main limitation in developing an analytical method for atmospheric ozone measurement is ozone's high reactivity. Ozone cannot be collected and preserved and for that reason there are no reference materials (RMs) in cylinders. Therefore, ozone standard concentrations must be generated dynamically *in situ*, either with (1) an ozone generator certified as an ozone transfer standard; or (2) an uncertified ozone generator whose output concentration levels are assayed with a primary standard photometer or an ozone assay instrument certified as an ozone transfer standard [16–19].

The US Environmental Protection Agency (US-EPA) and the National Institute of Standards and Technology (NIST) jointly developed a special, highly accurate standard photometer known as a Standard Reference Photometer (SRP) [20,21]. NIST maintains one "master" SRP, serial number 2 (SRP2) that serves as the US National Standard and a traveling SRP, serial number 0 (SRP0) that is used for intercomparison purposes. There are currently 22 other SRPs in use throughout the world. The Centro Nacional del Medio Ambiente (CENMA) maintains SRP serial number 45 (SRP45) which is a candidate to become the Chilean National Standard for ozone measurements.

In 2000 the International Bureau of Weights and Measures (BIPM, *Bureau international des poids et mesures*), in collaboration with the NIST, initiated a program to establish an international network for ozone reference standard comparisons and calibrations. Each SRP in the network is a standard in its own right and is not

* Corresponding author. Tel.: +56 2 978 73 70.
E-mail addresses: manleiva@uchile.cl, manleiva@me.com (M.A. Leiva G.).

0039-9140/$ – see front matter © 2011 Elsevier B.V. All rights reserved.
doi:10.1016/j.talanta.2011.08.006

"calibrated" against NIST or BIPM SRPs units. Instead, all SRPs are intercompared periodically to verify that they all agree with one another within a certain range and to establish traceability to the International System of Units (SI, Le Système international d'unités) [22,38].

Metrological traceability is formally defined as "property of a measurement result whereby the result can be related to a reference through a documented unbroken chain of calibrations, each contributing to the measurement uncertainty" [27]. The traceability of a measurement result is one of the most important issues to take care of when building up a measurement system from which reliable, internationally recognized results are expected [23–27]. In this sense the traceability to the SI ensures that the ozone measurements to be compared are independent of the time at which they are performed or of the organization performing the measurements. Traceability is crucial for producing global data sets that can be evaluated in terms of spatial and temporal trends and their uncertainties.

The SRPs can be used for certification of transfer standards, in order to keep the traceability chain unbroken. A transfer standard is a secondary standard that is used to transfer the accuracy of the SRP to the ozone analyzers at the monitoring sites. A transfer standard is first calibrated against the SRP and then used in the field to calibrate ozone analyzers [28]. In this way ozone monitoring results can be made traceable to the to SI. Fig. 1 represents the scheme that will be employed to ensure that the use of SRPs, and specifically the SRP45, ozone transfer standards and ozone analyzers are applied in a manner that will ensure a specified level of measurement uncertainty, traceability and accuracy.

Estimation of the uncertainty in the result of chemical measurements is an essential component of metrological traceability. In principle, all significant components of uncertainty must be identified and quantified [29–33]. While there are many existing protocols for analytical uncertainty estimation [34,35], it is important that the evaluation of the uncertainty of the measurements follows universal methods in order to establish the credibility of the measurements. The guide to the expression of uncertainty in measurement (GUM) is a key document used by National Measurement Institutes and industrial calibration laboratories as the basis for evaluating the uncertainty in the output of a measurement system [33].

To establish the formal metrological traceability of SRP45, a comparison method having a comprehensive uncertainty budget has been developed that is in accord with the principles of the GUM. The method includes a standard approach to uncertainty estimation through the definition of a model equation that relates all quantities influencing a particular measurement process.

2. Materials and methods

2.1. Standard reference photometer (SRP45)

Standard Reference Photometer SRP45 was constructed at NIST with the new measurement bias improvement components [20,21]. The upgrade was based on a study done by the BIPM and NIST and consists of a re-designed source/optics block to minimize transfer of heat from the source block to the gas in the absorption cells; and re-designed absorption cells made with approximately 3° angled windows to minimize repeated internal reflections between the cell windows and back reflections from the optical filters. The NIST glassblowing and optics shops fabricated a pair of quartz absorption cells made with optically sealed Suprasil #1. The focal length was also improved to provide a better collimated light signal with less divergence, and the two optical filters originally positioned at the exit of the absorption cells are now replaced with a single optical filter placed just after the collimating lens before the beam splitter, mirror, and absorption cells, see Fig. 2.

2.2. Ozone and zero-air generators

The UV technique requires a stable ozone generator, a UV photometer, and a source of clean, dry, pollutant-free at or below 1 nmol mol^{-1} ozone in the air. This clean air is typically termed pure-, reference-, or zero-air. A flowing (dynamic) system is set up in which the zero-air is passed through the ozone generator at a constant flow rate and discharged into a multiport manifold.

The SRP generator is based on the photolysis of oxygen molecules contained in purified air using radiation at 185 nm. The amount of ozone molecules produced depends on the intensity of the radiation and the rate of airflow. The rate of airflow is maintained at a constant value during a comparison, and the radiation intensity is varied to obtain a range of ozone mole fractions. The typical range over which measurements are carried out is 0.2–1000 nmol mol^{-1} of ozone in the air.

Ultrahigh pure air was supplied with a custom-built zero-air generator. Compressed air was first filtered and dehumidified with a combination of Nafion and heatless dryers and fed to a purification system consisting of a heating and oxidation unit and a series of adsorbents (charcoal, soda-lime and 4A molecular sieves). These purification processes remove trace gases including water vapor, non-methane hydrocarbons (NMHCs), NO, NO_2, SO_2, and CO present in air. The system is able to provide dry zero-air at up to 20 standard liters per minute. The zero-air output was pressure-controlled and supplied to the SRPs systems, as reference air. A portion of the zero-air was used to produce ozone for the direct intercomparison.

2.3. Comparisons procedure

The SRP45 was initially validated by comparison with the NIST Standard Reference Photometers, SRP2 and SRP0, with one serving as the US National Standard for ozone and the other as a traveling standard. Both SRP2 and SRP0 are traceable SI through measurements made at the BIPM as part of their global intercomparison program, BIPM.QM-K1 ozone at ambient level [36]. The period of validation was February 19 to March 5, 2010 and additional intercomparisons were done during the period May 5–10, 2010, just prior to shipment. Due to the 2010 earthquake in Chile, delivery of the SRP45 to CENMA was delayed by several months.

During all validation intercomparisons, one of the SRPs operated as host equipment and the other as guest equipment (SRP-Guest vs. SRP-Host). The SRP0 and SRP45 were operated as SRP-Guest to show the relationship between SRP0 and SRP45 vs. SRP2. The relationship between SRP0 vs. SRP45 was also obtained during these measurements in the NIST laboratory. The intercomparisons of SRP0 vs. SRP45 were subsequently conducted in the CENMA, to verify the results obtained at NIST. To evaluate whether a technical problem occurred during the round trip of SRP0 from NIST to CENMA to NIST, the relationship between SRP0 vs. SRP2 was verified. All of these results are shown in the present study.

Prior to the comparison, all the instruments were switched on and allowed to stabilize for at least 8 h. The pressure and temperature measurement systems of the instruments were checked at that time. No adjustments to any of the SRPs were necessary.

One comparison run included 10 different mole fractions distributed to cover the range, together with the measurement of reference air at the beginning and end of each run. The nominal mole fractions were measured in the 0, 200, 70, 420, 110, 300, 30, 350, 160, 500, 270 and 0 nmol mol^{-1} sequence imposed by the BIPM.QM-K1 key comparison protocol [37]. The result at each of

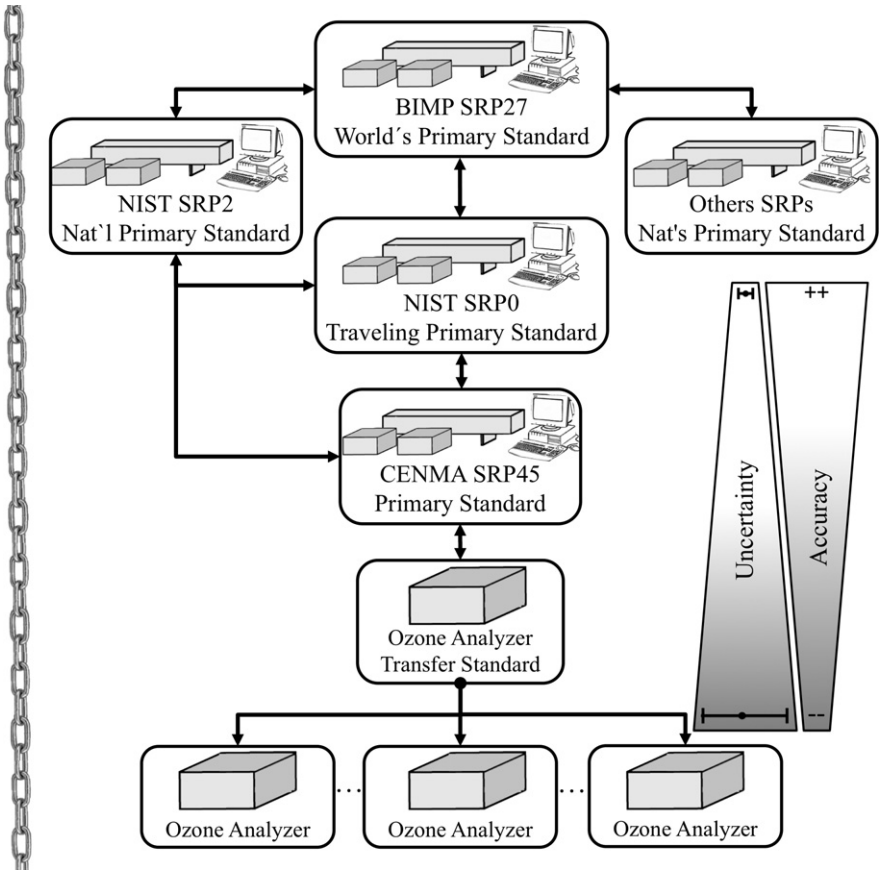

Fig. 1. Traceability chain of the SRPs, and of the SRP45 in particular.

these levels is an average of 10 single measurements. In all comparison runs sampling was done using a dual external manifold with 1-m sample and reference lines feeding into the inlet ports on each SRP allowing all instruments to sample the same gases from the same source manifolds. The source for the ozone sample and reference gas at NIST was from a customized Environics® Series 6100, computerized multi-gas calibration system, or ozone source was set from SRP45. The source for the ozone sample and reference gas in the CENMA laboratory was SRP45.

For each nominal value of the ozone mole fraction furnished by the ozone generator, the standard deviation ($\sigma_{SRP\text{-}Host}$) on the set of 10 consecutive measurements ($x_{ozone\,i}^{SRP-Host}$) recorded by

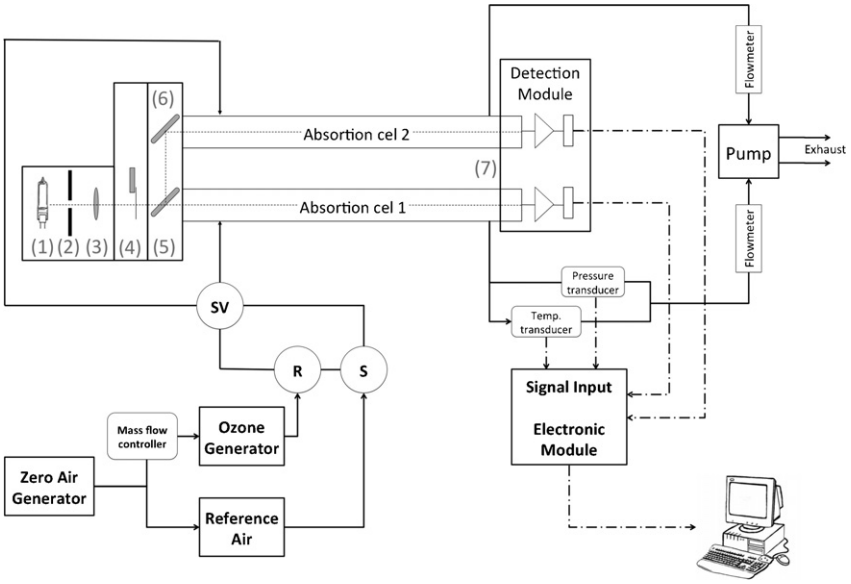

Fig. 2. Schematic of the SRP system. 1: mercury lamp; 2: aperture; 3: lens; 4: lamp shutter; 5: beam splitter; 6: mirror; SV: solenoid valve; R: reference manifold; S: sample manifold.

SRP-Host was calculated. The measurement results were considered valid if $\sigma_{SRP\text{-}Host}$ was less than 1 nmol mol^{-1}, which ensures that the photometers were measuring a stable ozone concentration. If not, another series of 10 consecutive measurements were performed.

The comparability between each SRP-Guest and the SRM-Host is evaluated by linear least squares regression as implemented in the software Standard Reference Photometer Control version 4.4.2 [38], according to:

$$x_{ozone}^{SRP-Guest} = a_0 + a_1 \times x_{ozone}^{SRP-Host} \quad (1)$$

where $x_{ozone}^{SRP-Guest}$ and $x_{ozone\,i}^{SRP-Host}$ correspond to a ozone concentration in nmol mol^{-1} measured by SRP-Guest and SRP-Host respectively; a_0 is an intercept, in nmol mol^{-1}, and a_1 is a slope.

2.4. Uncertainty estimation procedure

The procedure used to evaluate the uncertainty associated with the determination of the ozone concentration by UV photometry, and in concordance GUM [33], can be divided into the following steps:

(i) Description of the measurement procedures,
(ii) Specification and relationship between the measurand and the variables,
(iii) Identification of uncertainty sources,
(iv) Effect diagram and quantification of individual uncertainties,
(v) Calculation combined uncertainty,
(vi) Expanded uncertainty and
(vii) Expression of results.

2.4.1. Step 1: description of the measurement procedures

The measurement of ozone mole fraction by an SRP is based on the absorption of radiation at 253.7 nm by ozonized air in the gas cells of the instrument.

The SRP instrument design incorporates the use of two gas cells to overcome the instability of the light source, i.e., the SRP measures reference and sample air simultaneously using two absorption cells, then alternates the sample and reference gas to the cells. In the first part of the cycle, sample air is passed directly into cell 2 for measurement of the attenuated light intensity (Cell 2-I_{ozone}) and reference air is passed into cell 1 for the measurement of the reference light intensity at zero ozone concentration (Cell 1-I_{air}). In the second part of the cycle, sample air is passed directly into cell 1 for the measurement of the attenuated light intensity (Cell 1-I_{ozone}) and reference air is passed directly into cell 2 for the measurement of the reference light intensity at zero ozone concentration (Cell 2-I_{air}). The two half cycles are combined to calculate one single ozone concentration according to the Beer–Lambert law shown below. Thus, ozone in a sample stream can be measured continuously by alternately measuring the light level at the detectors ozone removed (reference) and then with ozone present (sample).

2.4.2. Step 2: specification of the measurand and relationship between the measurand and the variables

The measurement equation is derived from the Beer–Lambert and ideal gas laws. The number concentration of ozone (C_{ozone}), in molecules cm^{-3}, is calculated from:

$$C_{ozone} = -\frac{1}{2 \times \sigma \times L_{opt}} \times \frac{T}{T_{std}} \times \frac{P_{std}}{P} \times \ln(D) \quad (2)$$

where σ is the absorption cross-section of ozone at 253.7 nm in standard conditions of temperature (T_{std}; 273.15 K) and pressure (P_{std}; 101.325 kPa). The value used is: 1.1476×10^{-17} cm^2 mol^{-1} [36]; L_{opt} is the optical path length of one of the cells in cm; T is the measured temperature of the cells in K; P is the measured pressure of the cells in kPa; and D is the product of transmittances of two cells ($T_{r12} \times T_{r21}$), with the transmittance (T_{rij}) of one cell for each part of the cycle ($i = 1$ if $j = 2$ and $i = 2$ if $j = 1$) defined as:

$$T_{rij}|_{i=1;j=2\,\text{or}\,i=2;j=1} = \frac{I_{ozone\,i}}{I_{air\,j}} \quad (3)$$

where $T_{ozone\,i}$ is the UV radiation intensity measured from cell when containing ozonized air in cell i, and $I_{air\,j}$ is the radiation intensity measured from the cell when containing zero air in the cell j. In the case of UV radiation, intensity is corrected for disperse radiation and variation on the intensity of the light source.

Using the ideal gas law Eq. (2) can be recast in order to express the measurement results as a mole fraction (x_{ozone}) of ozone in the air:

$$x_{ozone} = -\frac{1}{2 \times \sigma \times L_{opt}} \times \frac{T}{P} \times \frac{R}{N_A} \times \ln(D) \quad (4)$$

where x_{ozone} is a measurement ozone concentration in nmol mol^{-1}; N_A is the Avagadro constant (6.022142×10^{23} mol^{-1}) and R is the gas constant (8.314472 J mol^{-1} K^{-1}).

The formulation implemented in the SRP software is:

$$x_{ozone} = -\frac{1}{2 \times \sigma_x \times L_{opt}} \times \frac{T}{T_{std}} \times \frac{P_{std}}{P} \times \ln(D) \quad (5)$$

where σ_x is the linear absorption coefficient at standard conditions, expressed in cm^{-1}, and linked to the absorption cross-section according to:

$$\sigma_x = \sigma \times \frac{N_A}{R} \quad (6)$$

2.4.3. Step 3 and 4: identification of uncertainty sources cause and effect diagram and quantification of individual uncertainties

An Ishikawa diagram or cause and effect diagram (sometimes also called fishbone diagram) is a useful tool to identify the influence parameters, i.e., the sources of uncertainty, of the whole procedure of ozone measurement. In this sense the sources of the uncertainty identified are: (a) optical path length (L_{opt}); (b) pressure (P); (c) temperature (T); (d) product of transmittances or intensity ratio of two cells (D) and (e) cross-section (σ). All of these influence parameters are showed in the cause and effect diagram in Fig. 3. Below we give a brief description of the source of uncertainty of these influence parameters.

(a) **Optical path length (L_{opt})**: The optical path is assumed to be identical to the total length of the two cells ($L_{opt} = L_{cell1} + L_{cell2} = 2L$). The exact value is dependent on the SRP serial number and these values are traceable to NIST measurements.

For the optical path length the source of uncertainty considered was three fold: reproducibility, measurement scale, and correction factor by light reflection in the cell. The following point briefly describes the estimation of uncertainty of these sources.

(i) *Reproducibility* ($\mu_{L_{opt\_oall}rep}$) : The uncertainty due to variations in overall cell length (L_{opt_oall}) can be estimated from a series of n independent measurement of cell path length. The standard deviation of these measurements is provided with the equipment by NIST. This can be used directly as a normally distributed standard uncertainty. The reproducibility can be estimated according to:

$$\mu_{L_{opt\_oall}rep} = \frac{s}{\sqrt{n}} \quad (7)$$

(ii) *Measurement scale* ($\mu_{L_{opt\_oall}scale}$) : A standard uncertainty is associated to the least significant digit of digital

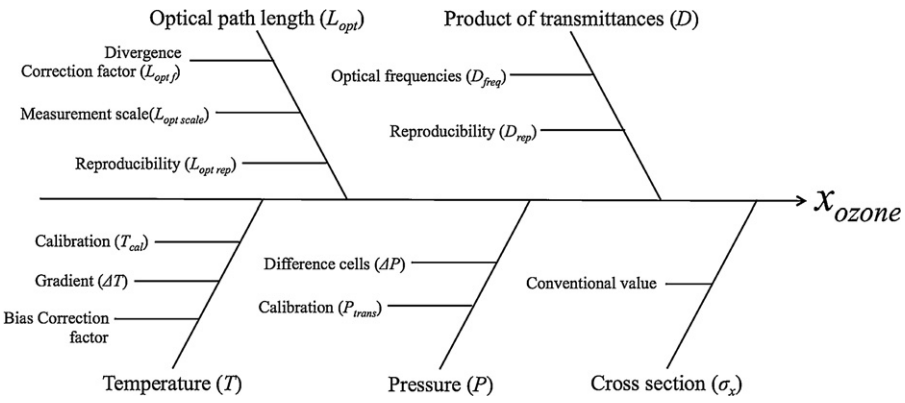

Fig. 3. The cause-effect diagram shows the main sources of uncertainty in a measurement of the ozone concentration with SRP equipment.

readout of the measuring instrument; assuming a triangular distribution.

$$\mu_{L_{opt-oall}scale} = \frac{accuracy}{\sqrt{3}} \tag{8}$$

(iii) *Thickness of each quartz window* ($\mu_{L_{opt}tn}$) : In order to calculate the L_{opt} (inside cell optical path length) it is necessary to know the thickness of the quartz windows in each cell. A standard uncertainty is associated to the tolerance of the measuring instrument; assuming a triangular distribution and estimated in a manner analogous to Eq. (8). This value is a measurement for each quartz window and is subtracted from the overall length measurement of each cell in order to estimate the optical path length.

(iv) *Correction factor by light reflection in the cell* ($\mu_{L_{optf}}$) : Is obtained from information provided in reference [21]. The standard uncertainty associated with light reflection in the cells (f) is deduced from a rectangular probability distribution, according to:

$$\mu_{L_{optf}} = \frac{5 \times 10^{-3} \times L_{opt}}{\sqrt{3}} \tag{9}$$

where 5×10^{-3} is an estimated bias.

The optical path length is then estimated from the difference of the average of the two cell measurements ($\bar{L}_{opt\_oall}$) and the thickness of the four cells ($L_{opt\_tn_i}$, $n = 1, 2, 3, 4$) according to

$$L_{opt} = 2 \times \bar{L}_{opt\_oall} - \sum_{i=1}^{4} L_{opt\_tn_i} \tag{10}$$

and the uncertainty associate to optical path length ($\mu_{L_{opt}}$) can be estimated according to:

$$\mu_{L_{opt}} = \sqrt{(2 \times \mu_{\bar{L}_{opt\_oall}})^2 + \sum_{i=1}^{4} (\mu_{L_{opt\_tn_i}})^2 + (\mu_{L_{opt}rep})^2 + (\mu_{L_{opt}scale})^2} \tag{11}$$

(b) **Pressure (*P*)**: Two sources of uncertainty were considered for pressure: transducer calibration and difference of pressure between the cells.

(i) *Transducer calibration* ($u_{P_{trans}}$) : The calibration certificate states that the relative uncertainty (RU) of the pressure transducer is ±0.05% of full scale. Assuming a rectangular distribution, the uncertainty associated with the calibration of the pressure transducer is:

$$u_{P_{trans}} = \frac{(RU/100) \times 101.325\,\text{kPa}}{\sqrt{3}} \tag{12}$$

(ii) *Difference of pressure between cells* ($\mu_{\Delta P}$): The SRP measurement equation assumes that the pressure is same in the two cells of the SRP during a measurement of ozone mole fraction, which takes 1 min, but these assumptions can be false and there may be a possible difference between the pressure in the two cells. Only one pressure transducer is located in one cell. For a given maximum pressure difference, $\Delta P_{\max}$, the uncertainty can be estimated:

$$\mu_{\Delta P} = \frac{\Delta P_{\max}/2}{\sqrt{3}} \tag{13}$$

The uncertainty associate to pressure (μ_P) can be estimated according to:

$$\mu_P = \sqrt{(\mu_{P_{trans}})^2 + (\mu_{\Delta P})^2} \tag{14}$$

(c) **Temperature (*T*)**: There are three sources of uncertainty for the T parameter: transducer calibration, gradient temperature in the cells, and *probe temperature bias*.

(i) *Transducer calibration* ($\mu_{T_{trans}}$) : The calibration certificate states that the temperature probe calibration has a maximum bias of ±0.15 K at 295 K, a usual work temperature condition. Assuming a rectangular probability distribution, the uncertainty for a given change in temperature, $\Delta T_{\max}$, is:

$$\mu_{T_{trans}} = \frac{\Delta T_{\max}}{\sqrt{3}} \tag{15}$$

(ii) *Gradient temperature in the cells* ($\mu_{T_{grad}}$) : The cells have several heat sources within the instrument (notably the UV lamp housing and the pneumatic valves) which could influence the temperature along the gas stream. Experimental measurements at the BIPM experimental studies showed that the temperature of the gas flowing in the gas cell is uniform within ±0.1 K ($\Delta T_{grad}/2$), at controller room temperature conditions, at 295 K [21]. Assuming a rectangular probability distribution the uncertainty of gradient temperature in the cell can be estimated in the same way as Eq. (12), and considering the value provide from BIMP its possible estimate a ΔT_{grad} equal to 2×0.1 K. All measurements were done.

(iii) *Correction factor by temperature probe bias* ($f_{T_{bias}}$) : A temperature bias correction has been added based on the assumption that the temperature measurement can be over-estimated by as much as 0.3 °C. Calculations were made at the approximate ozone mole fractions of 77 nmol mol^{-1} and 436 nmol mol^{-1} to show the effect of a −0.3 °C temperature correction [21]. The results at both mole fractions were used to determine an offset

of −0.1%. This bias correction of −0.001 nmol mol^{-1} was computed after the combined standard uncertainty equation.The uncertainty associate to temperature (μ_T) can be estimated according to:

$$\mu_T = \sqrt{(\mu_{T_{trans}})^2 + (\mu_{T_{grad}})^2} \quad (16)$$

(d) **Product of transmittances or intensity ratio of two cells (*D*)**: For the product of transmittances or intensity ratio of two cells (D), there are two sources to consider: a reproducibility and uncertainty of the optical frequencies used to calculate D or scalar resolution.

(i) *Reproducibility* ($\mu_{D_{rep}}$) : These uncertainties are estimated from the standard deviation of several measurements and assume a normal probability distribution; according to Eq. (7). This quantity has been estimated from the standard deviation ($s_{D_{rep}}$) of $n = 100$ measurement of this ratio with no flow of reference air or ozone/air mixtures within the cells.

(ii) *Optical frequencies used to calculate D* ($\mu_{D_{Frec}}$) : It is derived from the uncertainty of the optical frequencies used to calculate D. The value of this standard uncertainty is obtained from bibliography data and assumes a triangular probability distribution.

The uncertainty associate to optical frequencies (μ_D) can be estimated according to:

$$\mu_D = \sqrt{(\mu_{D_{\mathrm{rep}}})^2 + (\mu_{D_{\mathrm{frec}}})^2} \quad (17)$$

(e) **Cross-section (σ_x)**: The ozone absorption cross-section at 253.65 nm has a relative uncertainty (μ_{σ_x}) of 2.12% at a 95% level of confidence [36]. However, all ozone photometers use the same conventional value, and thus the uncertainty can be set to zero when considering the comparability of two instruments [21,38–40].

2.4.4. Step 5–7: calculation combined uncertainty, expanded uncertainty and expression of results

For each main source of the uncertainty (μ_{q_i}), i.e., temperature (T), pressure (P), cross-section (σ_x), the product of transmittances or intensity ratio of two cells (D) and the optical path length (L_{opt}), it is possible to calculate the combined standard uncertainty in function of the i-sources identified ($\mu_{s_{q_i}}$), according to:

$$\mu_{q_i} = \sqrt{\sum_{i=1}^{n} (\mu_{s_{q_i}})^2} \quad (18)$$

The combined standard uncertainty for the ozone concentration measurement, calculated according to the model above is given by Eq. (5), and can be estimated by:

$$\mu^2_{x_{ozone}} = \sum_{i=1}^{n} \left(\frac{\partial f(q_1, q_2, \ldots, q_n)}{\partial q_i|_{qi=T,P,\sigma_x,D,L_{opt}}} \right) \times \mu^2_{q_i}|_{q_i=T,P,\sigma_x,D,L_{opt}} = \sum_{i=1}^{n} c_i^2 \times \mu^2_{q_i} \quad (19)$$

where $(\partial f(q_1, q_2, \ldots, q_n))/(\partial q_i|_{q_i=T,P,\sigma_x,D,L_{opt}})$ is a sensitivity coefficient (c_i), and corresponds to the according Eq. (19) for each variable:

$$\frac{\partial x_{ozone}}{\partial L_{opt}} = \frac{1}{2 \times \sigma_x \times L_{opt}^2} \times \frac{T}{T_{std}} \times \frac{P_{std}}{P} \times \ln(D) = -\frac{x_{ozone}}{L_{opt}} \quad (20)$$

$$\frac{\partial x_{ozone}}{\partial T} = \frac{1}{2 \times \sigma_x \times L_{opt}} \times \frac{1}{T_{std}} \times \frac{P_{std}}{P} \times \ln(D) = -\frac{x_{ozone}}{T}$$

$$\frac{\partial x_{ozone}}{\partial P} = \frac{1}{2 \times \sigma_x \times L_{opt}} \times \frac{T}{T_{std}} \times \frac{P_{std}}{P^2} \times \ln(D) = -\frac{x_{ozone}}{P} \quad (21)$$

$$\frac{\partial x_{ozone}}{\partial D} = \frac{1}{2 \times \sigma_x \times L_{opt}} \times \frac{T}{T_{std}} \times \frac{P_{std}}{P} \times \frac{1}{D} = -\frac{x_{ozone}}{D \times \ln(D)} \quad (22)$$

$$\frac{\partial x_{ozone}}{\partial \sigma_x} = \frac{1}{2 \times \sigma_x^2 \times L_{opt}} \times \frac{T}{T_{std}} \times \frac{P_{std}}{P} \times \frac{1}{D} = -\frac{x_{ozone}}{\sigma_x} \quad (23)$$

The combined standard uncertainty can be written:

$$\mu_{x_{ozone}} = x_{ozone} \times \sqrt{\left(\frac{\mu_{\sigma_x}}{\sigma_x}\right)^2 + \left(\frac{\mu_{L_{opt}}}{L_{opt}}\right)^2 + \left(\frac{\mu_T}{T}\right)^2 + \left(\frac{\mu_P}{P}\right)^2 + \left(\frac{\mu_D}{D \times \ln(D)}\right)^2} \quad (24)$$

The uncertainty associated with the ratio of intensities (μ_D) is assumed constant on the range of ozone mole fractions and can be written:

$$\mu_D = \frac{\mu(D) \times x_{ozone}}{D \times \ln(D)} = \frac{\mu(D) \times B}{D} \approx \mu(D) \times B \quad (25)$$

where D can be approximated by 1 for the entire range and B is a constant term and the combined standard uncertainty can be rewritten:

$$u_{x_{ozone}} = x_{ozone} \times \sqrt{\left(\frac{u_{\sigma_x}}{\sigma_x}\right)^2 + \left(\frac{u_{L_{opt}}}{L_{opt}}\right)^2 + \left(\frac{u_T}{T}\right)^2 + \left(\frac{u_P}{P}\right)^2 + (u_D \times B)^2} \quad (26)$$

The final results should be stated together with the expanded uncertainty (U_{ozone}), calculated using a coverage factor (κ), which gives a level of confidence according to:

$$U_{ozone} = \kappa \times u_{x_{ozone}} \quad (27)$$

At the end the following form is recommended to express the result:

$$x_{ozone} \pm U_{ozone}(\text{units}) \quad (28)$$

3. Results and discussion

3.1. Comparability

The comparability between SRP0, SRP45 vs. SRP2 and SRP45 vs. SRP0 was evaluated during the installation process after, before and at CENMA in order to diagnose if there are any changes in the performance of SRP0 during transit to and from NIST has occurred.

Fig. 4a and b and Table 1 show time series of the slopes and intercepts measurement and statistics results the SRP45 and SRP0 against to SRP2. The results of the fifth data sets (that correspond to 159 runs) reveal that the SRP0 and SRP2 gives comparable intercept and slope results and is basically identical before and after transit to CENMA and not change in the performance are revealed. SRP45 are comparable to SRP2 and both are comparable to SRP0.

Fig. 4c and d and Table 1 show time series of the comparison of the SRP45 referenced to the SRP0 measurement at NIST and CENMA laboratories. The result of the five data sets (that correspond to 54 runs) showed a good agreement relationship between the SRP45 and the SRP0 has not changed during transit of SRP45 and SRP0 from NIST to CENMA. These result will be possible authenticate the validations results of SRP45.

Fig. 5 and Table 2 list the results of the comparison between SRP45 and SRP0 and correspond to twenty six data sets (270 runs) at different ozone level measurement. A good correlation between SRP45 vs. SRP2, is within the acceptable range of 1.00 ± 0.01 (slope), and 0.0 ± 0.5 nmol mol^{-1} (intercept) for an SRP and constitutes official validation of SRP45 [41].

Table 3 lists the regression results for SRP45 vs. SRP2 measurement in different days. The data shown the repeatability of the slopes and intercept is acceptable within the BIMP.QM-K1 criteria [37,40].

In order to compare the measurement results of the SRP45 with the worldwide SRP, we used the data obtained from the key comparison BIPM.QM-K1. The BIPM.QM-K1 project is aimed at evaluating the level of comparability of ozone reference standards

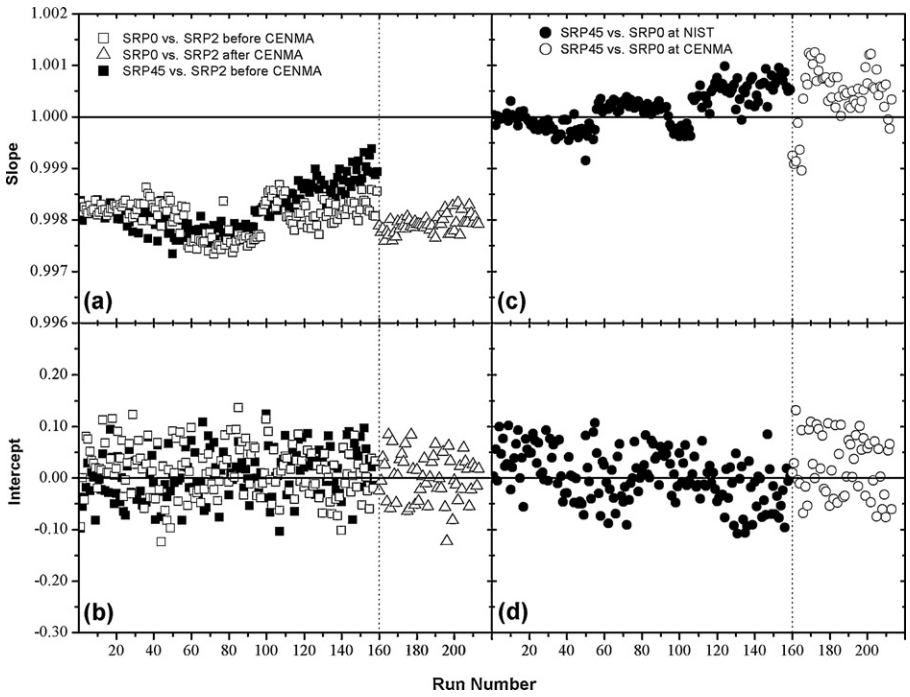

Fig. 4. Results of comparisons among three SRPs. The NIST SRP0 and the CENMA SRP45 are referenced to the NIST SRP2 at the NIST laboratory before installation of SRP45 and are cross-referenced during the installation. The results shown are (a) slopes and (b) intercepts of SRP45 (solid squares) and SRP0 (open squares) versus SRP2. The vertical dashed line denotes the measurement run after the installation at the NIST laboratory of the SRP0 vs. SRP2. The figure (c) slopes and (d) intercepts of SRP0 versus SRP35 before (solid circle) and after (open circle) the installation. The vertical dashes denote installation of SRP45 at the CENMA laboratory.

Table 1
Linear regressions statistical of comparability result between SRP0, SRP45 vs. SRP2 and SRP45 vs. SRP0 was evaluated during the installation process after, before after and at CENMA location.

	SRP-Guest vs. SRP-Host location	Fig. 4 and symbol	Runs number	Slope (adim)				Intercept (nmol mol^{-1})			
				$a_{1,mean}$	$a_{1,max}$	$a_{1,min}$	σ_{a_1}	$a_{0,mean}$	$a_{0,max}$	$a_{0,min}$	σ_{a_0}
1	SRP45 vs. SRP2 before CENMA	a and b ■	159	0.99805	0.99868	0.99733	0.00033	0.00883	0.12367	−0.10391	0.04743
2	SRP0 vs. SRP2 before CENMA	a and b □	159	0.99821	0.99938	0.99734	0.00042	0.01228	0.13622	−0.12429	0.04993
3	SRP0 vs. SRP2 after CENMA	a and b ○	54	0.99792	0.99834	0.99759	0.00017	0.00157	0.08456	−0.12256	0.04563
4	SRP45 vs. SRP0 before CENMA	c and d ▲	159	1.00015	1.00098	0.99915	0.00036	0.00315	0.10709	−0.10789	0.05018
5	SRP45 vs. SRP0 at CENMA	c and d △	54	1.00043	1.00125	0.99896	0.00054	0.02253	0.13156	−0.07636	0.05909

$a_{1,i}$: slope mean, maximum and minimum; σ_{a1} : standard deviation of slope; $a_{0,i}$: intercept mean, maximum and minimum; σ_{a_0} : intercept standard deviation.

that are maintained as national standards, or as primary standards within international networks for ambient ozone measurements (BIPM.QM-K1, 2007). Fig. 6 showed the degrees of equivalence of the SRP45 to the international standard (data from BIPM.QM-K1 key comparison): (a) nominal value of 80 nmol mol^{-1}; (b) nominal value of 420 nmol mol^{-1}. The results indicate that the SRP45 are comparable at two levels of concentration with the reported results of the other SRPs.

Table 2
Results of the validation between SRP45 and SRP0 in nmol mol^{-1}.

$x_{ozone}^{nominal}$	$x_{ozone,mean}^{SRP0}$	$x_{ozone,max}^{SRP0}$	$x_{ozone,min}^{SRP0}$	$\sigma_{SRP0}^{x_i}$	$\bar{x}_{ozone,mean}^{SRP45}$	$x_{ozone,max}^{SRP45}$	$x_{ozone,min}^{SRP45}$	$\sigma_{SRP45}^{x_i}$
0	0.03	0	−0.1	0.1	0.04	0	−0.1	0.7
30	28.3	30.2	25.0	0.1	28.3	25.0	25.0	0.4
70	70.6	73.1	64.3	0.2	70.5	64.2	64.2	0.1
110	110.9	113.9	104.7	0.2	110.9	104.4	104.4	0.2
160	159.9	162.2	155.8	0.2	160.0	155.6	155.6	0.4
210	209.8	215.3	193.9	0.2	209.6	193.7	193.7	0.1
260	258.7	259.7	255.6	0.2	258.6	255.6	255.6	0.4
300	307.2	312.4	298.5	0.1	307.0	298.1	298.1	0.1
350	354.9	360.7	349.5	0.4	354.6	349.1	349.1	0.4
420	418.4	425.7	407.0	0.4	418.2	406.9	406.9	0.2
480	479.3	484.3	480.2	0.4	479.1	479.9	479.9	0.1
0	0.01	0	−0.1	0.6	0.02	0	−0.1	0.2

$x_{ozone}^{nominal}$: ozone nominal concentration; $x_{ozone,mean}^{SRP0}$: average ozone concentration in SRP0; $x_{ozone,max}^{SRP0}$: maximum ozone concentration in SRP0; $x_{ozone,min}^{SRP0}$: minimum ozone concentration in SRP0; $\sigma_{SRP0}^{x_i}$: standard deviation ozone concentration SRP0; $\bar{x}_{ozone,mean}^{SRP45}$: average ozone concentration in SRP45; $x_{ozone,max}^{SRP45}$: maximum ozone concentration in SRP45; $x_{ozone,min}^{SRP45}$: minimum ozone concentration in SRP45; $\sigma_{SRP45}^{x_i}$: standard deviation ozone concentration SRP45.

Table 3
Repeatability study of the slopes and intercept measurement at different days.

Day i	Slope (adim)				Intercept (nmol mol^{-1})			
	$a_{1,mean}^{Day_i}$	$a_1^{Day_i}$	$a_{1,\min}^{Day_i}$	$\sigma_{a_1}^{Day_i}$	$\bar{a}_{0,mean}^{Day_i}$	$a_{0,\max}^{Day_i}$	$a_{0,\min}^{Day_i}$	$\sigma_{a_0}^{Day_i}$
1	0.99971	1.00035	0.99899	0.00017	0.01	0.1315	0.0680	0.04810
2	1.00078	1.01680	1.00069	0.00034	0.02	0.1093	0.0007	0.07418
3	1.00029	1.00077	1.00030	0.00024	0.02	0.1065	0.0538	0.06052

$a_{1,mean}^{Day_i}$: slope average day i; $a_{1,\max}^{Day_i}$: slope maximum day i; $a_{1,\min}^{Day_i}$: slope minimum day i; $\sigma_{a_1}^{Day_i}$: standard deviation slope day i; $\bar{a}_{0,mean}^{Day_i}$: intercept average day i; $a_{0,\max}^{Day_i}$: intercept maximum day i; $a_{0,\min}^{Day_i}$: intercept minimum day i; $\sigma_{a_0}^{Day_i}$: standard deviation intercept day i.

3.2. Quantification of individual uncertainties

a. **Optical path length uncertainty** ($u_{L_{opt}}$): The cell length was measured using a Coordinate Measuring Machine (CMM) with a manufacturer stated accuracy of ±0.00866 mm. Taking this value and using Eq. (8), the uncertainty of measurement scale is 0.0005 cm.

Nine independent measurements were made around the perimeter of each cell. This data was used to determine the average value and overall uncertainty of the cell lengths, according to Eq. (7). Each cell has an independent cell length, but the two cell lengths were averaged to produce one single cell length that is used in the calculation of ozone mole fractions using the SRP control software. The results obtained from these measurements were 90.017 and 90.005 cm with a standard deviation of 0.006 and 0.007, for cells 1 and 2, respectively.

The thickness of each quartz window was measured using a caliper with a tolerance of 0.0025 cm, which the uncertainty of the thickness of each quartz window is 0.0014 cm. The result of the thickness of each cell was a 0.163 and 0.163 for the two windows of cell 1, and 0.163 and 0.166 for the two windows of cell 2.

The NIST SRP upgrade improves this bias so that the path length correction is no longer necessary, but since there is still a known divergence of the light as it proceeds through the length of the cells, the true actual path length is not known without further research. Therefore, the same standard uncertainty of 0.52 cm used in the bias study will be used here to account for the divergence of the light in the cells, according to Eq. (9). This is a conservative approach as this uncertainty was a combined estimate that included the multiple reflections within the cells as well as any light divergence. Further research may lead to a lower estimated uncertainty for the actual path length.

The data used for estimating the optical path length are presented in Table 3. The final average optical path length and uncertainty for the SRP45 absorption cells are 89.68 ± 0.004 cm (Table 4).

b. **Pressure (*P*)**: The pressure transducer has been calibrated with a stated relative uncertainty of ±0.05% at full scale. Assuming a

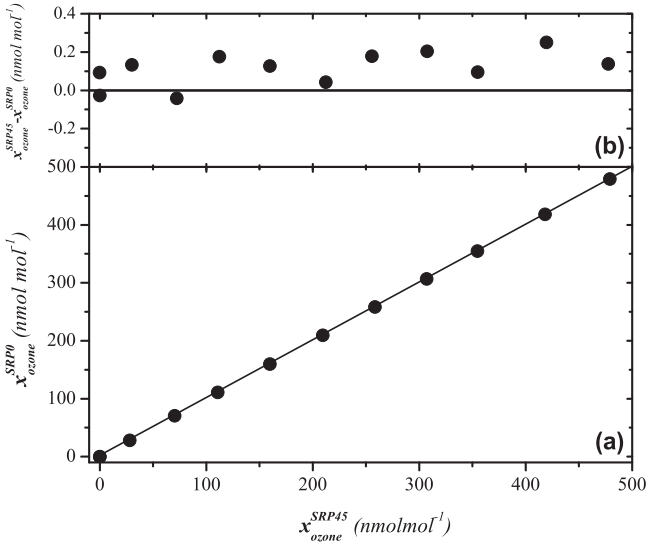

Fig. 5. Scatter plots of the ozone mole fractions of CENMA SRP45 against SRP0 at CENMA laboratory. The solid line is a linear regression line (a) and residual (b).

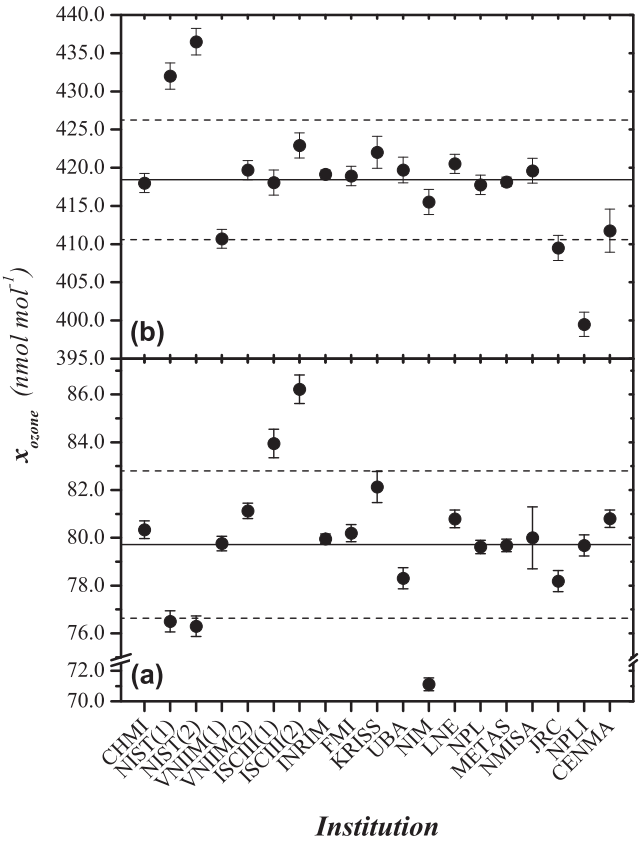

Fig. 6. Degrees of equivalence of the SRP45 to the international standard (data from BIPM.QM-K1 key comparison), (a) nominal value of 80 nmol mol^{-1}; (b) nominal value of 420 nmol mol^{-1}. The solid line indicates the average of the all ozone measurements and the dash line is a one standard deviation of the average. (List of participant is available online at: http://www.bipm.org/en/scientific/chem/gas_metrology/ozone_comparisons.html). *Acronyms*: CZECH Hydrometeorological Institute, Czech Republic (CHMI); National Institute of Standards and Technology, USA (NIST); D.I. Mendeleev Institute for Metrology, Russia (VNIIM); Instituto de Salud Carlos III, Spain (SCIII); Instituto Nazionale di Ricerca Metrologica, Italy (INRIM); Finnish Meteorological Institute, Finland (FMI); Korea Research Institute of Standards and Science, Korea (KRISS); Federal Environmental Agency, Germany (UBA); Van Swinden Laboratorium B.V., Nederland (NMi); Métrologie Chimique LCSQA, France (LNE); National Physical Laboratory, United Kingdom (NPL); Federal Office of Metrology, Switzerland (METAS); National Metrology Institute of South Africa, South Africa (NMISA); Joint Research Center, European Commission (JRC); National Physical Laboratory, United Kingdom (NPL); Centro Nacional del Medio Ambiente, Chile (CENMA).

Table 4
Uncertainty budget for concentration of SRP45.

Component, q_i	Source, s_j	Distribution	Standard uncertainty, u_{s_j}	Combined standard uncertainty, u_{q_i}	Sensitivity coefficient, c_i	Contribution by source, $\lvert c_i\rvert \times u_{std}^{com}$
L_{opt} (cm)	Reproducibility	Normal	0.002	0.052	$-(x_{ozone}/L_{opt})$	$5.79\times10^{-4}\times x_{ozone}$
	Measurement scale	Rectangular	0.0005			
	Correction factor	Rectangular	0.052			
P (kPa)	Reproducibility	Normal	1.50×10^{-2}	0.023	$-(x_{ozone}/P)$	$2.46\times10^{-4}\times x_{ozone}$
	Calibration transductor	Rectangular	6.69×10^{-13}			
	Difference cells	Rectangular	1.70×10^{-2}			
T (K)	Reproducibility	Normal	5.13×10^{-13}	0.065	x_{ozone}/T	$2.20\times10^{-4}\times x_{ozone}$
	Calibration transductor	Rectangular	3.00×10^{-2}			
	Gradient	Rectangular	5.80×10^{-2}			
D (adim)	Reproducibility	Normal	5.66×10^{-6}	9.80×10^{-6}	$x_{ozone}/(D\times \ln(D))$	$2.28\times x_{ozone}$
	Optical frequencies	Rectangular	0.000			
σ_x ($cm^2\ mol^{-1}$)	Conventional value	Triangular	1.15×10^{-17}	–	$-(x_{ozone}/\sigma_x)$	$1.06\times10^{-2}\times x_{ozone}$

rectangular probability distribution, according to Eq. (11), this corresponds to a standard uncertainty of 0.029 kPa.

In order to determine the difference in pressure of each cell of SRP45, the pressure is measured in cell 1 taking readings for valve l on, then valve 2 on, followed by the same measurements when measuring the pressure of cell 2. This process is done followed by adjustments to the valves (if necessary) until the pressure difference is less than or equal to 0.06 kPa. Assuming a triangular distribution, the uncertainty of the difference of pressure, according to Eq. (12), is 0.017 kPa.

c. **Temperature (*T*)**: The SRP temperature measurement is done using a platinum temperature sensor (RTD), which is mounted underneath the optical bench measuring the gas passing through a small manifold just after exiting cell 1. The RTD probe itself has a manufacturer stated uncertainty of 0.15 °C at 25 °C (298.15 K), which produces a standard uncertainty of 0.029 K, according to Eq. (13). The temperature gradient bias upgrade source/optics block and shutter cover reduces the temperature gradient below 0.l °C, assuming the temperature gradient is no more than 0.1 °C and a rectangular distribution leads to a standard uncertainty of 0.058 K. The additional temperature probe heating effect has not been independently measured by NIST and therefore no corrections have been made. Therefore, an additional bias correction has been added based on the assumption that the temperature measurement can be over-estimated by as much as 0.3 °C. Calculations were made at the approximate ozone mole fractions of 77 nmol mol^{-1} and 436 nmol mol^{-1} to show the effect of a −0.3 °C temperature correction. The results at both mole fractions were used to determine an offset of 0.1%.

d. **Product of transmittances or intensity ratio of two cells (*D*)**: The SRP resolution scaler uncertainty is 6×10^{-6}. In addition, the repeatability of the SRP scalers operating without any ozone sample is measured using the "stability multimonitor" diagnostic collecting 100 minor ratios. Then, 99 major ratios or "double ratios" are calculated from the minor ratios. From this data, the maximum absolute difference from the average major ratio is found and assuming the data follows a triangular distribution, the standard uncertainty is calculated. The scaler data used to estimate the product of transmittances or intensity ratio of two cells at 0 nmol mol^{-1} was 1.024, 1.02379, 1.02377 and 5.66×10^{-6} for scaler mean, scaler maximum and minimum, and standard deviation of the scaler respectability. The final value of product of transmittances or intensity ratio of two cells and uncertainty for the SRP45 under the validation process was 0.22.

e. **Cross-section (σ_x)**: The ozone absorption cross-section at 253.65 nm has been defined by a number of research groups. The results were evaluated by the NIST, and the conclusion was reached at a value of $1.147\times10^{-21}\ m^2\ mol^{-1}$ (or $30.4\ kPa^{-1}\ m^{-1} = 308.32\ atm^{-1}\ cm^{-1}$). It is directly traceable to SI units [38,39]. The relative uncertainty of 2.12% at a 95% level of confidence is considered. This is the best estimate for the absorption cross-section to be used with the SRP, and thus the uncertainty can be set to zero when considering the comparability of two instruments.

3.3. Uncertainty budgets

The different components of the uncertainty are reported in a budget form in Table 4. The contributions, nominally uncorrelated, have been quadratically summed and expressed in nmol mol^{-1}.

The combined standard uncertainty to the SRP45 is:

$$\mu_{x_{ozone}}(x_{ozone}) = \left[\sqrt{(0.27)^2 + (1.18\times10^{-2}\times x_{ozone})^2}\right]\ \text{nmol mol}^{-1} \quad (29)$$

Removing the absorption cross-section uncertainty, the equation becomes:

$$\mu_{x_{ozone}}(x_{ozone}) = \left[\sqrt{(0.27)^2 + (1.19\times10^{-3}\times x_{ozone})^2}\right]\ \text{nmol mol}^{-1} \quad (30)$$

Fig. 7 shows the propagated uncertainty of the SRP45 as a function of ozone mole fraction. If the uncertainty from the absorption cross-section is not considered, the combined standard uncertainty

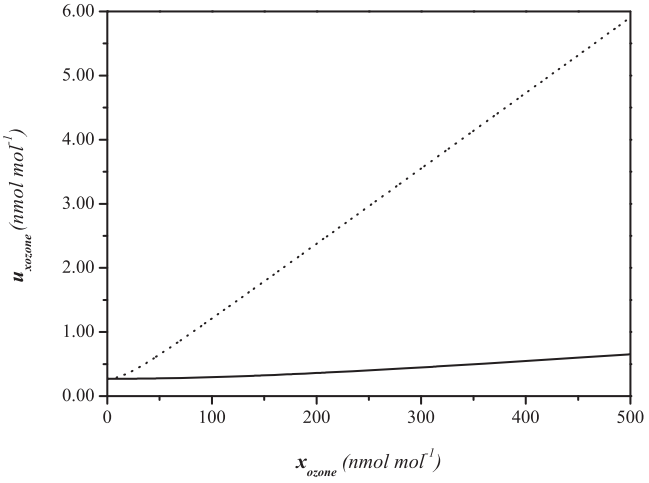

Fig. 7. Standard uncertainty ($k = 1$) associated with one measurement result of SRP45, with (a) and without (b) the absorption cross-section uncertainty component.

in the SRP45 has a weak dependence on the ozone mole fraction. The uncertainty in the range of the concentration of ozone from 0 to 100 nmol mol^{-1} is 0.7 nmol mol^{-1} and in the range from 100 to 500 nmol mol^{-1} is 0.7%.

The uncertainty, i.e., a deviation range (or interval) from a reported measurement result, with corresponding probability, may be evaluated, but it is not possible to obtain a perfect (error-free) measurement, nor it is possible to estimate an uncertainty with absolute certainty. However, under well-controlled conditions and a well-understood measurement process and procedure, it is possible to minimize and estimate reasonably well (at high probability) the uncertainties of measured quantities and the final measurement result.

This summarizes the above uncertainty budget for SRP45 without the absorption cross-section uncertainty or excluding the temperature probe heating bias. Without the temperature probe bias, the 95% level of confidence expanded uncertainty and considering that the effective number of degrees of freedom for all the components is large, the conventional 95% coverage factor (κ) of 2 is appropriate. The expanded uncertainty is:

$$U_{95\%} = [2 \times \mu_{x_{ozone}}(x_{ozone})]\ \text{nmol mol}^{-1} \quad (31)$$

With the temperature probe bias, the 95% level of confidence expanded and a coverage factor (κ) of 2 the uncertainty is:

$$U_{95\%}^{T_{bias}} = [2 \times \mu_{x_{ozone}}(x_{ozone}) - (0.001 \times x_{ozone})]\ \text{nmol mol}^{-1} \quad (32)$$

If an independent calibration of the SRP45 temperature probe is done and the SRP temperature measurement is offset before actual measurements are performed, this additional temperature probe bias is not required. The temperature measurement offset can be done using the SRP control software, or by simply offsetting the temperature span point when using the temperature calibrator.

The expanded uncertainty interval, without the absorption cross-section uncertainty or the temperature probe heating bias, at a level of confidence of 95% calculated using a coverage factor $\kappa = 2$, is:

$$x_{ozone} \pm U_{95\%} = x_{ozone} \pm 2 \times \left[\sqrt{(0.27)^2 + (1.18 \times 10^{-2} \times x_{ozone})^2}\right]\ \text{nmol mol}^{-1} \quad (33)$$

4. Conclusions

This paper has presented a detailed measurement equation and developed a full uncertainty budget for the analysis of ozone measurement in the SRP equipment. The results of the estimations of the overall expanded uncertainty of the measurements are useful for the purpose of analyzing the ozone by SRP. The comparisons were also in excellent agreement and these results demonstrated that the SRP45 is equivalent to both NIST SRPs and, through SRP2, SRP45 is comparable to international network of SRPs.

From averaging the values for the slope and intercepts from the nine validation data sets obtained at NIST of SRP 45 vs. SRP 2, the following equation is derived and will serve as the official results for the validation of SRP45:

$$x_{ozone}^{SRP45} = [0.013 + 0.00806 x_{ozone}^{SRP2}]\ \text{nmol mol}^{-1} \quad (34)$$

The examination of the uncertainty budget has revealed that:

- The largest contribution to the combined uncertainty is from the uncertainty of the absorption cross-section. However, this source is only important for comparing measurements made SRPs with those made using other analytical systems.
- If the uncertainty of the absorption cross-section is not consider, the main contribution to uncertainty that is the product of transmittances or intensity ratio of two cells (D). This reveals the importance of taking SRP instrumental condition into account in uncertainty estimation.
- The final value of product of transmittances or intensity ratio of two cells and uncertainty for the SRP45 under the validation process was 0.22. That is lower than the BIPM-NIST estimate of 0.28.
- The propagated uncertainty of the SRP45 as a function of ozone mole fraction. If the uncertainty from the absorption cross-section is not considered, the combined standard uncertainty in the SRP45 has a weak dependence on the ozone mole fraction.

Acknowledgements

The financial support of the Chilean Ministry of the Environment (Ministerio del Medio Ambiente, MMA), is gratefully acknowledged for the implementation of the SRP Lab in CENMA. This effort was conducted under the MMA-CENMA 2008–2010 agreement. The authors are grateful to Dr. Raúl G.E. Morales S. for his helpful discussions and comments. I would also like to thank the anonymous reviewers for their useful recommendations that improved this manuscript.

References

[1] R. Vingarzan, Atmos. Environ. 38 (2004) 3431.
[2] M.J. Molina, L.T. Molina, J. Air Waste Manage. Assoc. 54 (2004) 644.
[3] M. Lacasana-Navarro, C. Aguilar-Garduno, I. Romieu, Salud Publica Mex. 41 (1999) 203.
[4] Y. Sadanaga, J. Matsumoto, Y. Kajii, J. Photochem. Photobiol. C 4 (2003) 85–104.
[5] J.M. Azevedo, F.L.T. Goncalves, M.D. Andrade, Int. J. Biometeorol. 55 (2011) 187.
[6] N.E. Selin, S. Wu, K.M. Nam, J.M. Reilly, S. Paltsev, R.G. Prinn, M.D. Webster, Environ. Res. Lett. 4 (2009), doi:10.1088/1748-9326/4/4/044014.
[7] M. Iriti, F. Faoro, Water Air Soil Pollut. 187 (2008) 285.
[8] A. Screpanti, A. De Marco, Environ. Pollut. 157 (2009) 1513.
[9] EPA, List of Designated Reference and Equivalent Methods, Office of Air Quality Planning and Standards Air Quality Assessment Division, Research Triangle Park, North Carolina, 2011, http://www.epa.gov/ttn/amtic/criteria.html.
[10] ASTM-D5110-98, Standard Practice for Calibration of Ozone Monitors and Certification of Ozone Transfer Standards Using Ultraviolet Photometry, American Society for Testing of Materials (ASTM), West Conshohocken, Pennsylvania, 2010.
[11] EPA, Quality Assurance Handbook for Air Pollution Measurement Systems, vol. II: Ambient Air Quality Monitoring Program, Office of Air Quality Planning and Standards Air Quality Assessment Division, Research Triangle Park, North Carolina, 2008, http://www.epa.gov/ttn/amtic/files/ambient/pm25/qa/QA-Handbook-Vol-II.pdf.
[12] ISO13964, Air Quality – Determination of Ozone in Ambient Air – Ultraviolet Photometric Method, International Organisation for Standardisation, Geneva, Switzerland, 1998.
[13] L. Zhang, D.J. Jacob, X. Liu, J.A. Logan, K. Chance, A. Eldering, B.R. Bojkov, Atmos. Chem. Phys. 10 (2010) 4725.
[14] EPA, Transfer Standards for Calibration of Air Monitoring Analyzers for Ozone. Technical Assistance Document, Office of Air Quality Planning and Standards Air Quality Assessment Division, Research Triangle Park, North Carolina, 2010, http://www.epa.gov/ttn/amtic/files/ambient/qaqc/OzoneTransferStandardGuidance.pdf.
[15] L. Konopelko, I. Nekhlioudov, V. Chelibanov, Metrologia 34 (1997) 97.
[16] B. Buchmann, J. Klausen, C. Zellweger, Chimia 63 (2009) 657.
[17] ISO20988 (2007), International Organisation for Standardisation, Geneva, Switzerland.
[18] ASTM-D5011-92 (1992), Standard Practices for Calibration of Ozone Monitors using Transfer Standards, American Society for Testing of Materials (ASTM), West Conshohocken, Pennsylvania, 2009.
[19] H. Tanimoto, H. Mukai, S. Hashimoto, J.E. Norris, J. Geophys. Res. Atmos. 111 (2006) D16313, doi:10.1029/2005JD006983.
[20] BIPM-2010/07, Upgrade of the BIPM Standard Reference Photometers for Ozone and the Effect on the On-going Key Comparison BIPM.QM-K1, 2010. <http://www.bipm.org/utils/common/pdf/rapportBIPM/2010/07.pdf>.
[21] J. Viallon, P. Moussay, J.E. Norris, F.R. Guenther, R.I. Wielgosz, Metrologia 43 (2006) 441.
[22] The International System of Units (SI), Organisation Intergouvernementale de la Convention du Mètre 8th edition, 2006. <http://www.bipm.org/utils/common/pdf/si_brochure_8.pdf>.
[23] G.P. Eppeldauer, M. Racz, Appl. Optics 43 (2004) 2621.
[24] R.I. Wielgosz, R. Kaarls, Chimia 63 (2009) 606.
[25] H. Tanimoto, H. Mukai, Y. Sawa, H. Matsueda, S. Yonemura, T. Wang, S. Poon, A. Wong, G. Lee, J.Y. Jung, K.R. Kim, M.H. Lee, N.H. Lin, J.L. Wang, C.F. Ou-Yang, C.F. Wu, H. Akimoto, P. Pochanart, K. Tsuboi, H. Doi, C. Zellwegern, J. Klausenn, J. Environ. Monitor. 9 (2007) 1183.

[26] N. Ridler, B. Lee, J. Martens, K. Wong, IEEE Microw. Magn. 8 (2007) 44.
[27] JCGM 200:2008, International Vocabulary of Metrology – Basic and General Concepts and Associated Terms (VIM), Joint Committee for Guides in Metrology, 2008, http://www.bipm.org/en/publications/guides/vim.html.
[28] ISO15337, Ambient Air – Gas Phase Titration – Calibration of Analysers for Ozone, International Organisation for Standardisation, Geneva, Switzerland, 2009.
[29] ISO/IEC17025, General Requirements for the Competence of Testing and Calibration Laboratories, International Organisation for Standardisation, Geneva, Switzerland, 2005.
[30] L. Kirkup, Eur. J. Phys. 23 (2002) 483.
[31] L. Deldossi, D. Zappa, Accredit. Qual. Assur. 14 (2009) 159.
[32] W. Kessel, Thermochim. Acta 382 (2002) 1.
[33] JCGM 100, Evaluation of Measurement Data – Guide to the Expression of Uncertainty in Measurement, Joint Committee for Guides in Metrology, 2008, http://www.bipm.org/en/publications/guides/gum.html.
[34] M. Priel, Accredit. Qual. Assur. 14 (2009) 235.
[35] EUROLAB, EUROLAB Technical Secretariat – EUROLAB, European Federation of National Associations of Measurement, Testing and Analytical Laboratories, Paris, France, 2007.
[36] J. Viallon, P. Moussay, R. Wielgosz, J.E. Norris, F. Guenther, Metrologia 45 (2008) 08008.
[37] J. Viallon, Protocol for the Key Comparison BIPM.QM-K1, Ozone at ambient level Bureau.
[38] NIST/SRP-CS, NIST Ozone Standard Reference Photometer Control Software, Version 4.41, 2010. http://www.nist.gov/mml/analytical/gas/SRPpage.cfm.
[39] A.G. Hearn, Proc. Phys. Soc. 78 (1961) 932.
[40] BIPM.QM-K1, International Comparisons of Ozone Standards, 2011. <http://kcdb.bipm.org/appendixB/KCDB_ApB_result.asp?cmp_idy=733&cmp_cod=BIPM%2EQM%2DK1&search=2&cmp_cod_search=bipm%2Eqm%2Dk1&page=1&met_idy=&bra_idy=&epo_idy=&cmt_idy=&ett_idy_org=&cou_cod=>.
[41] NIST Report of Analysis: Validation of NIST Standard Reference Photometer, serial number 45, August 2010.